Journal of Thermal Analysis and Calorimetry (2019) 138:1259–1267
https://doi.org/10.1007/s10973-019-08247-z

Synergistic flame-retardant effects of ammonium polyphosphate and AC-Fe_2O_3 in epoxy resin

Qingyi Song[1] · Hongjuan Wu[2] · Hao Liu[1] · Xiaoxia Han[1] · Hongqiang Qu[1] · Jianzhong Xu[1]

Received: 18 October 2018 / Accepted: 8 April 2019 / Published online: 27 April 2019

Abstract

The synergistic flame-retardant and smoke suppression properties of ammonium polyphosphate (APP) and activated carbon-supported Fe_2O_3 (AC-Fe_2O_3) on flame-retardant epoxy resin (EP) composites were studied. The fire behavior and smoke emission of EP composites were evaluated by limiting oxygen index (LOI), scanning electron microscopy, UL-94 vertical burning, and cone calorimeter test. LOI and UL-94 tests showed that the addition of appropriate amount of AC-Fe_2O_3 can effectively reduce the fly ash phenomenon, the dripping, and after-flame time. The thermogravimetric analysis and derivative thermogravimetry results showed that APP and AC-Fe_2O_3 can effectively decrease the maximum decomposition rate (R_{max}) and promote the carbonization reaction of EP. As for the cone calorimeter test results, APP and AC-Fe_2O_3 clearly changed the decomposition behavior of EP, leading to the formation of a stable char layer on the surface of the composites. When flame-retardant loading was 4 mass%, the peak heat release rate and peak smoke production rate of the 3APP/1AC-Fe_2O_3/EP sample decreased 50.2% and 46.9%, respectively. The amount of char residual after test increased from 8.47 to 21.25%. In addition, it was observed from the macroscopic photographs of the char residue after the cone test that, at the optimum proportion, APP and AC-Fe_2O_3 could promote the formation of compact charred layers and prevent their cracking, which effectively protected the underlying materials from burning.

Keywords Flame retardant · Smoke suppression · EP · APP · Activated carbon

Introduction

The flammability of epoxy resin (EP) is its potential fire hazard. When it is ignited, the fire spreads rapidly, and great volumes of toxic fumes, such as carbon monoxide, aromatic compounds, and hydrocarbons, will be concomitantly released [1, 2]. This result not only endangers human health, but also hinders the rescue of people in the fire. Therefore, it is an urgent social demand to study the combustion mechanism and flame-retardant treatment of EP.

At present, ammonium polyphosphate (APP) is one of widely used inorganic phosphorus flame retardant. APP has a neutral pH, high P, N content, low price, and dual function of acid source and gas source. However, the addition of 9 mass% APP will enable the EP vertical combustion rating to pass V-0. Moreover, APP has high hygroscopicity, which leads to a decrease in the mechanical properties of the material. Therefore, the synergistic agent is often added to achieve the purpose of improving the flame-retardant efficiency of APP.

In recent years, more and more carbon-based flame retardants have been researched. Yue et al. [3] applied expandable graphite (EG) and APP together to improve the flame retardancy of EP, confirming that joint use of EG and APP can not only increase the limiting oxygen index (LOI) but also improve the anti-dropping performance and char

Electronic supplementary material The online version of this article (https://doi.org/10.1007/s10973-019-08247-z) contains supplementary material, which is available to authorized users.

✉ Hongqiang Qu
hqqu@163.com

✉ Jianzhong Xu

[1] Key Laboratory of Analytical Science and Technology of Hebei Province, The Flame Retardant Materials and Processing Technology Engineering Technology Research Center, College of Chemistry and Environmental Science, Hebei University, Baoding 071002, Hebei, People's Republic of China

[2] Department of Foundation Couses, Agricultural University of Hebei, Cangzhou 061100, People's Republic of China

layer quality of EP. Zhang et al. [4] used activated carbon spheres (ACs) as a synergistic flame retardant for APP, and adding 0.1% of ACs and 2.9% of APP can make EP pass V-0 level in the vertical combustion test. Wang et al. [5] prepared the bamboo-based porous carbon materials and used it as synergistic agent for APP flame-retardant EP, and the results showed that the porous carbon materials can improve the thermal stability of the flame-retardant EP, catalyze the thermal degradation of APP to release NH_3 and H_2O, accelerate the cross-linking and char formation, and promote the formation of pyrophosphate during the thermal degradation. In addition, AC can also be used for flame-retardant treatment of other polymer systems and can be used as synergistic agent for molybdenum oxide in improving the flame retardancy of poly(vinyl chloride) [6]. Gong et al. [7] demonstrated that the use of activated carbon and Ni_2O_3 in the flame-retardant polypropylene (PP) can greatly increase its thermal stability, and carbon nanotubes are generated in situ during combustion, which can be used as a flame heat shield and reduce the release of flammable degradation products of PP.

Transition metal elements have good flame-retardant and smoke-suppressing effects, and transition metal oxides are typical ones which can be used as synergistic agent for APP to improve the flame retardancy of the polymer materials [8]. Chen et al. [9] confirmed that Fe_2O_3 can promote the early cross-linking of the polymer in the decomposition process and increase the smoke suppression efficiency and thermal degradation temperature of the intumescent flame retardant. Fe element could enhance the thermal stability of the intumescent flame-retardant PP system (IFR-PP) at high temperatures and effectively increase the char residue formation. Our previous work has shown that the distribution of Fe_2O_3 in polymer matrix can be effectively enhanced by the loading of Fe_2O_3 to activated carbon (AC-Fe_2O_3) [10]. The activated carbon which was synthesized using cattail and H_3PO_4 as raw material can not only improve the dispersion property of Fe_2O_3 but also has a good synergistic effect on flame retardant and smoke suppression with Fe_2O_3.

This study was designed to explore whether the AC-Fe_2O_3 can be prepared as an additive-type flame retardant and had a synergistic effect with APP on enhancing the flame retardancy and reducing the smoke release of EP. Herein, m-phenylenediamine was selected as the curing agent for EP, and APP was used as the intumescent flame retardant. AC-Fe_2O_3 was used as the synergistic flame retardant to prepare the multi-component intumescent flame-retardant system. The thermal degradation and combustion of APP and AC-Fe_2O_3 were investigated by means of LOI, thermogravimetric analysis (TG), differential thermogravimetric (DTG), cone calorimetry (CONE), char residual morphology, and X-ray powder diffraction (XRD) analysis.

Experimental

The granular activated carbon composite (AC-Fe_2O_3) was synthesized in our laboratory based on activated carbon (prepared from cattail) and iron oxalate [10]. Commercial ammonium polyphosphate (APP, form II, polymerization degree $\geq$ 1000) was supplied by Shifang Taifeng New Flame Retardant Co., Ltd. (Sichuan, China). M-phenylenediamine (MPD, AR grade) was obtained from Bluestar Chemical New Material Co., Ltd. (Tianjin, China). EP was purchased from Chengdu Kelong Chemical Reagent Co., Ltd. (Chengdu, China). Solvents applied in this study were all analytical grade and used directly.

Preparation of flame-retarded epoxy composites

Formulations of flame-retarded EP composites are shown in Table 1. EP was dried in an oven at 60 °C for 4 h before using. EP composites were prepared by mixing EP (100 g) with designed amounts of milled APP and AC-Fe_2O_3 in a Brabender mixer at 60 °C for 0.5 h and then added the curing agent MPD, magnetic stirring for 30 min, poured the evenly mixed EP into the mold, pre-cured for 2 h in an oven at 80 °C, continue curing at 150 °C for 3 h 40 min, and took out the sample after cooling naturally. The resultant samples were designated as xAPP/yAC-Fe_2O_3/EP, where x and y represented the mass percentages of APP and AC-Fe_2O_3 in the composites, respectively. The prepared samples were sequentially recorded as EP, 4APP/EP, 3APP/1AC-Fe_2O_3/EP, 2APP/2AC-Fe_2O_3/EP, 1APP/3AC-Fe_2O_3/EP, 4AC-Fe_2O_3/EP.

Characterization

The morphology of the char layers and section after impact test were observed by scanning electron microscopy (SEM). SEM images were obtained using a Phenom scanning electron microscope (Phenom, GER) with an acceleration voltage of 10 kV. The surfaces of samples were sprayed on a thin gold layer before the observation.

The char layers after cone calorimetry test were tested using a D8-ADVANCE X-ray diffraction analyzer (Bruker, GER). Tested samples were examined with Cu Ka ray γ = 0.15406 nm, radiant tube voltage = 40 kV, and the current = 40 mA.

The limiting oxygen index (LOI) measurement was conducted using an PX-05-005 oxygen index instrument (PHINIX, China) according to ASTM D 2863-2010. The sample was burned at room temperature under air

Table 1 Formulations of flame-retarded EP composites

Sample	Sample name	EP/g	MPD/g	APP/g	AC-Fe_2O_3/g
1#	EP	100	11	–	–
2#	4APP/EP	100	11	4	–
3#	3APP/1AC-Fe_2O_3/EP	100	11	3	1
4#	2APP/2AC-Fe_2O_3/EP	100	11	2	2
5#	1APP/3AC-Fe_2O_3/EP	100	11	1	3
6#	4AC-Fe_2O_3/EP	100	11	–	4

atmosphere. The size of the specimens was 130 mm × 6.5 mm × 3.2 mm.

The vertical burning test (UL-94) was performed using a CZF-3 instrument (Jiangning, China) according to ANST/UL94-2010. The dimension of the sample was 125 mm × 12.5 mm × 3.2 mm.

TG was performed on a TG-449C instrument (NETZSCH, GER). The tested samples were heated from 35 to 700 °C at a heating rate of 10 °C min^{-1} under a dynamic nitrogen flow of 50 mL min^{-1}. Masses of these samples were kept within 7 ~ 8 mg in an open Al_2O_3 pan.

The cone calorimeter tests were performed on an Icone Plus Cone calorimeter (Fire Testing Technology, UK) according to ISO 5660 standard procedures. Each specimen with dimensions of 100 mm × 100 mm × 3 mm was wrapped in aluminum foil and exposed horizontally to an external heat flux of 50 kW m^{-2}.

The mechanical properties of specimens were tested using both tensile and impact tests. The tensile properties were tested by a UTM4204 universal tensile testing machine (SUNS, China) at a tensile rate of 20 mm min^{-1} according to ISO 3167: 2002 standard procedures. The impact properties were performed on a JJ-20 pendulum impact tester (Changchun, China) at a pendulum specification of 15 J according to ISO 180: 2000 standard procedures.

Results and discussion

The LOI and UL-94 tests

The flame retardancy of the epoxy composites was evaluated via LOI and UL-94 vertical burning tests, and the data of samples 1#–6# are summarized in Table 2.

During the combustion process, the LOI of neat EP was very low (25.3%) with a large amount of black smoke and pungent odor. In the UL-94 test, the neat EP burned violently and dripped severely. The drippings ignited the underlying absorbent cotton and caused re-ignition [11]. The LOI value of EP can be improved to a certain extent via the incorporation of APP and AC-Fe_2O_3. The LOI value and UL-94 rating of sample 2# significantly increased to 28.3% and V-1 level with less smoke and no dripping.

After replacing APP with 1, 2, 3, and 4 parts of AC-Fe_2O_3, respectively, the LOI value of samples dropped from 28.0 to 27.0%. This result indicates that adding a small amount of AC-Fe_2O_3 has little effect on the LOI value. However, in UL-94 test, sample 3# can pass V-0 level. This is mainly because transition metal oxides have good flame-retardant and smoke-suppressing effects. AC-Fe_2O_3 can improve the thermal stability of the flame-retardant EP, catalyze the thermal degradation of APP to release NH_3 and H_2O, accelerate the cross-linking and char formation. Therefore, adding appropriate amount of AC-Fe_2O_3 can effectively reduce the after-flame time, resulting in improved flame retardancy of the epoxy matrix.

Table 2 The LOI and UL-94 test data of epoxy composites

Sample	Sample name	LOI/%	UL-94			
			t_1/s	t_2/s	Dripping	Rating
1#	EP	25.3	–	–	Y	NO
2#	4APP/EP	28.3	10.2	17.0	N	V-1
3#	3APP/1AC-Fe_2O_3/EP	28.0	4.3	5.4	N	V-0
4#	2APP/2AC-Fe_2O_3/EP	27.5	12.6	15.8	N	V-1
5#	1APP/3AC-Fe_2O_3/EP	27.5	38.9	86.8	N	NO
6#	4AC-Fe_2O_3/EP	27.0	–	–	Y	NO

Thermal performance

In order to further study the effect of the synergistic effect of AC-Fe_2O_3 and APP on the thermal degradation of the EP samples, we performed a thermogravimetric test on the above samples under nitrogen atmosphere [12].

The TG–DTG curves and related data for pure epoxy and flame-retardant epoxy resins are presented in Fig. 1 and Table 3, respectively, including the initial decomposition temperature at 5% mass loss ($T_{5\%}$), the maximum decomposition rate (R_{max}), the temperature at the maximum decomposition rate (T_{max}), and the residue mass at 800 °C.

It can be observed from Fig. 1 that the EP contains one strong (300–500 °C) mass loss process under nitrogen condition. The mass loss at this stage is due to the fracture of the epoxy resin molecular network. The temperature at 5% mass loss ($T_{5\%}$, taken as the onset of the degradation) of EP is 367.8 °C. The maximum mass loss temperature of EP is 376.2 °C, and only 14.6% char residue remains at 800 °C. After the addition of the flame retardant, the thermal degradation of the flame-retarded EP sample did not change substantially, but it was apparent that the initial decomposition temperature was decreased and the char residues of all the composites at 800 °C were increased.

In sample 2#, after adding 4 mass% APP, the $T_{5\%}$ of the EP sample was significantly advanced (34 °C), and the char residue at 800 °C was significantly increased. This is due to the fact that the polyphosphoric acid (PPA) which produced by the decomposition of APP can catalyze the thermal cracking and cross-linking of EP [13], thus leading to an advance in the $T_{5\%}$ of the system and an increase in the char residual content. In sample 6#, after adding 4 mass% AC-Fe_2O_3, the R_{max} of the flame-retarded EP sample was reduced from − 20.4 to − 15.4% °C^{-1}, compared with the neat EP. This is because AC can act as an excellent insulation material to increase the stability of the char layer [13, 14]. In the later stage of combustion, the char residue is not easily lost by re-pyrolysis. In sample 3#, after 1 mass% APP was replaced by 1 mass% AC-Fe_2O_3, the $T_{5\%}$ of the sample was slightly delayed compared with that of sample 2#, and the char residue at 800 °C slightly increased. After increasing the amount of AC-Fe_2O_3, though $T_{5\%}$ is more delayed, it is still ahead of the sample 1#. This is because as the amount of AC increases, the physical barrier effect of the carbon source becomes more pronounced [15].

Table 3 TG and DTG data for EP composites at 10 °C min^{-1} under nitrogen atmosphere

Sample	$T_{5\%}$/°C	R_{max}/%/°C	T_{max}/°C	Residue at 800 °C/ mass%
1#	367.8	− 20.4	376.2	14.8
2#	334.4	− 15.4	345.4	24.0
3#	336.8	− 14.0	347.5	24.3
4#	338.7	− 12.6	351.3	23.6
5#	342.9	− 11.3	375.9	20.5
6#	351.9	− 15.4	364.5	19.6

In the mass loss rate curves (Fig. 1b), we can see that the R_{max} of samples 3#–5# is lower than that of samples 2# and 6#, and with the increase in AC-Fe_2O_3 addition, R_{max} gradually decreased. These results due to that Fe_2O_3 which is AC-Fe_2O_3 can promote the thermal decomposition of APP to remove NH_3 and H_2O in advance, and generate polyphosphoric acid compounds [16, 17]. At the same time, the formation of Fe–O–P bonds can promote the cross-link curing of polyphosphoric acid compounds during the post-combustion period [18], so the quality of the char layer is improved. In addition, AC is an excellent physical barrier carbon source, can not only play a role in insulating and blocking oxygen, but also can increase the amount of char residual.

In summary, the addition of the flame retardant makes the $T_{5\%}$, the decomposition rate, and the char residual content of the epoxy resin change. APP plays a catalytic role in carbonization, AC-Fe_2O_3 plays a dual role of physical barrier and catalytic degradation, and both can act as a synergistic dual flame retardant for epoxy resins. On

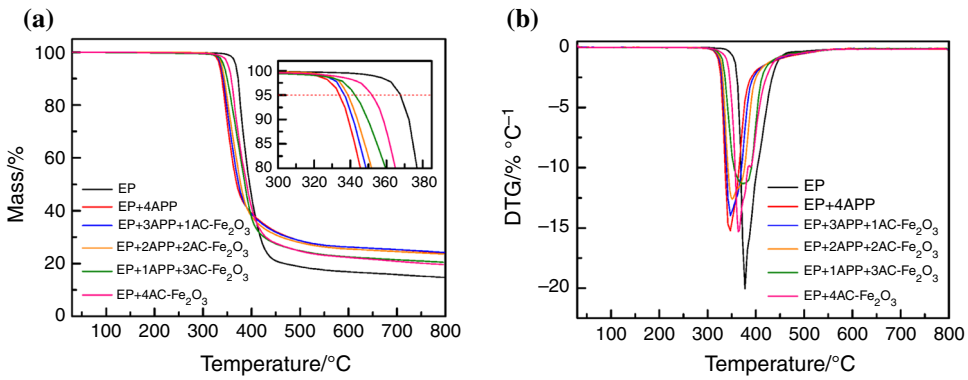

Fig. 1 TG (**a**) and DTG (**b**) curves for EP composites at 10 °C min^{-1} under nitrogen atmosphere

one hand, in the initial stage of EP pyrolysis, APP decomposes to form PPA. This kind of phosphoric acid can promote the degradation of EP and generate a more stable carbon layer, which plays a role in heat insulation and oxygen isolation. On the other hand, the physical barrier of AC can prevent the degradation products from volatilizing and escaping. The presence of Fe element also promotes the decomposition of APP, which significantly improves the carbonization of EP flame-retardant materials.

The char morphology analysis

In order to gain more detailed information about the microstructure of the residual chars from EP composites after combustion at 800 °C, SEM observations were conducted and the results are shown in Fig. 2.

From Fig. 2, we can see that there are many collapses and holes in the char residue of sample 1#. These holes are conducive to the diffusion of flammable gas and fly ash in the combustion, so that the sample will continue to burn without quenching; a lot of toxic gases and smoke are produced, which is not conducive to the escape and evacuation of fire personnel. Correspondingly, the structure of the sample 2#–6# char residue is more stable and has fewer holes.

In Fig. 2b, APP causes the EP sample to generate an intumescent char residue. However, this porous structure has a low strength and a low melt viscosity. In the late stage of combustion, it can easily be destroyed by pyrolysis, which is not conducive to the extinguishing of the flame during combustion. In Fig. 2f, after adding 4 parts of AC-Fe_2O_3, the char residue structure is continuous with few holes. In Fig. 2c, the char residue of the EP sample with both APP and AC-Fe_2O_3 added has characteristic of char residual when both are added separately. This indicates that replacing 1 mass% APP with 1 mass% AC-Fe_2O_3 resulted in the polymer to form an intumescent char residue during combustion. This char surface is dense and plays a good role in heat insulation and oxygen isolation.

In addition to the presence of intumescent char layers, the char residue structure becomes denser, which can reduce the heat conduction and mass transfer of the sample and protect the unburned area [19].

Taking into account the LOI, UL-94, and thermogravimetric data of the above flame-retarded EP samples, sample 3# (with three APPs and one AC-Fe_2O_3 added) was selected as the best ratio flame-retarded EP sample.

Cone calorimeter measurement

Cone calorimeter measurement is one of methods for effectively simulating the actual fire behavior. Herein, cone calorimeter results such as heat release rate (HRR), total heat release (THR), smoke release rate (SPR), and total smoke emission (TSR) can reflect the flame retardancy, smoke suppression, and toxicity reduction in the flame-retardant EP composites [20, 21].

The HRR and THR curves of neat EP, 4APP/EP, 3APP/1AC-Fe_2O_3/EP and 4AC-Fe_2O_3/EP (1#–3# and 6#) are shown in Fig. 3. The corresponding data obtained from cone calorimetry are presented in Table 4. The macroscopic images of char residue are shown in Fig. 4.

Figure 3a and b shows the HRR curves of neat EP, 4APP/EP, 3APP/1AC-Fe_2O_3/EP, and 4 AC-Fe_2O_3/EP. The HRR curve of pure EP displays a high and sharp peak with a peak value (PHRR) of 1298.08 kW m^{-2} in the whole combustion. Compared with pure EP, the PHRR of all the

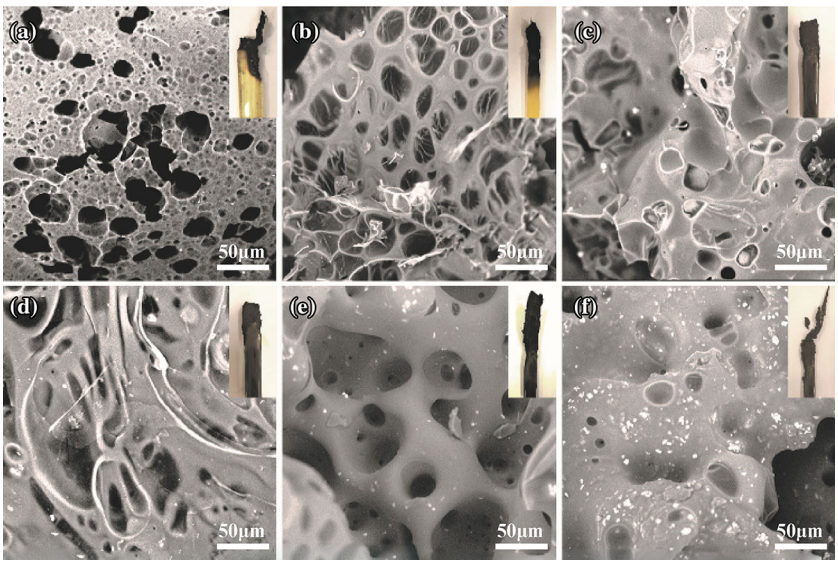

Fig. 2 SEM images of the residual chars after combustion at 800 °C from neat PP (**a**), 4APP/EP (**b**), 3APP/1AC-Fe_2O_3/EP (**c**), 2APP/2AC-Fe_2O_3/EP (**d**), 1APP/3AC-Fe_2O_3/EP (**e**) and 4AC-Fe_2O_3/EP (**f**)

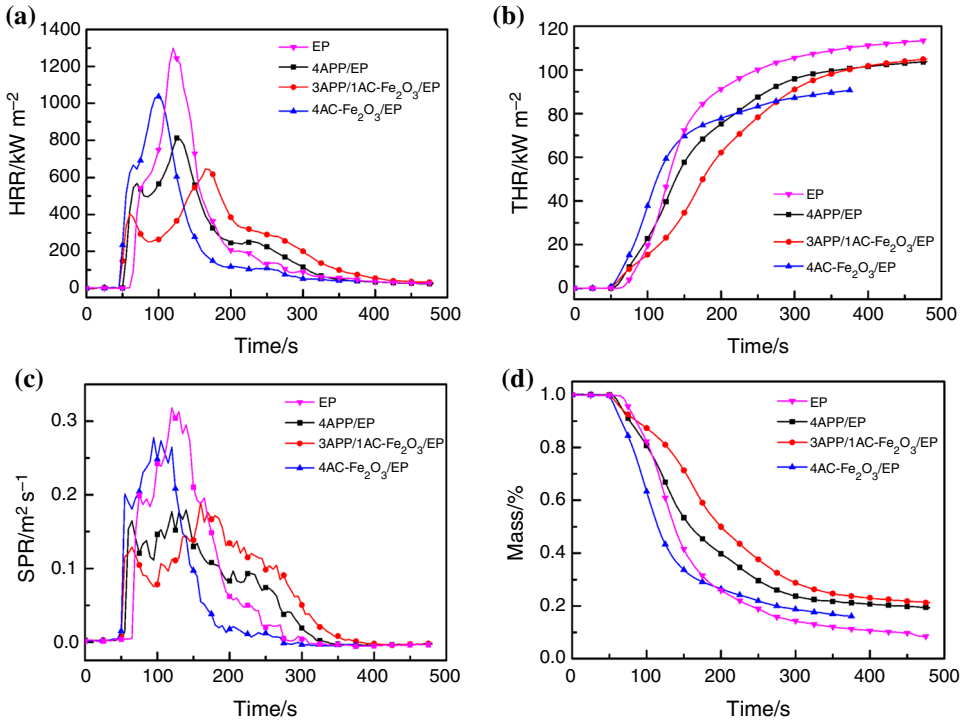

Fig. 3 Curves for EP composites in cone calorimeter: HRR (**a**), THR (**b**), SPR (**c**) and mass (**d**)

Table 4 Data for EP composites in cone calorimeter at an external radiant flux of 50 kW m^{-2}

Item	1#	2#	3#	6#
TTI/s	65	55	53	49
PHRR kW m^{-2}	1298.08	811.54	646.41	1036.80
t_{PHRR}/s	120	125	165	100
Av-HRR/kW m^{-2}	275.87	243.15	243.17	276.71
THR/MJ m^{-2}	113.11	103.34	104.55	90.52
PSPR/m^2 s^{-1}	0.32	0.18	0.17	0.27
TSP/m^2	30.17	26.01	30.30	23.39
Av-MLR/g s^{-1}	0.091	0.081	0.083	0.088
Residue/%	8.47	19.35	21.25	16.07

flame-retardant EP composites has decreased. When 4 mass% APP was added, the PHRR decreased by 37.5%. This is mainly because of the APP, which can form ammonia and polymeric phosphoric acid. The ammonia and polymeric phosphoric acid can act as a protective layer of high molecular polymer and isolate oxygen. 4AC-Fe_2O_3/EP also shows good performance by a decreased value of 20.2% compared with pure EP. This phenomenon ascribed to the function of AC and Fe_2O_3. AC can act as an excellent carbon source, and Fe_2O_3 can promote the early cross-linking of the polymer in the decomposition process. So, it can form a compact char layer which can prevent the release of heat. After replacing 1 mass% APP with 1 mass% AC-Fe_2O_3, the PHRR of EP composites dropped more than the pure EP (50.2%). It is noteworthy that compared with 4APP/EP and 4AC-Fe_2O_3/EP, 3APP/1AC-Fe_2O_3/EP shows an interesting phenomenon in the heat release curve: The second heat release peak is delayed and is gentler. This may be attributed to that APP and AC-Fe_2O_3 act synergistically to form char residue, making the char layer produced in the first thermal degradation stage of better quality and less likely to be destroyed in the subsequent combustion process [22].

Figure 3b shows the total heat release rate (THR) curve of EP and its composites. For pure EP, the THR curve increases obviously sharply than that of other samples. Different from the pure EP, after 300 s of irradiation, the THR curves of flame-retardant EP composites keep growing slowly. This is due to the fact that the residue will continue to oxidize and decompose under high radiant power. It is particularly noteworthy that the slope of the THR curve of 3APP/1AC-Fe_2O_3/EP was significantly lower than 4APP/EP before 200 s. This shows that in the pre-combustion stage of EP, a more stable char layer was formed, which blocked the propagation of heat. Combined with the HRR results, we can conclude that 3APP/1AC-Fe_2O_3/EP is more efficient than APP or AC-Fe_2O_3 alone to reduce heat release.

Figure 3c shows the smoke production rate (SPR) curve of EP and its composites. It can be seen that the peak SPR (PSPR) of three flame-retardant EP samples decrease remarkably compared to pure EP. This indicates that APP,

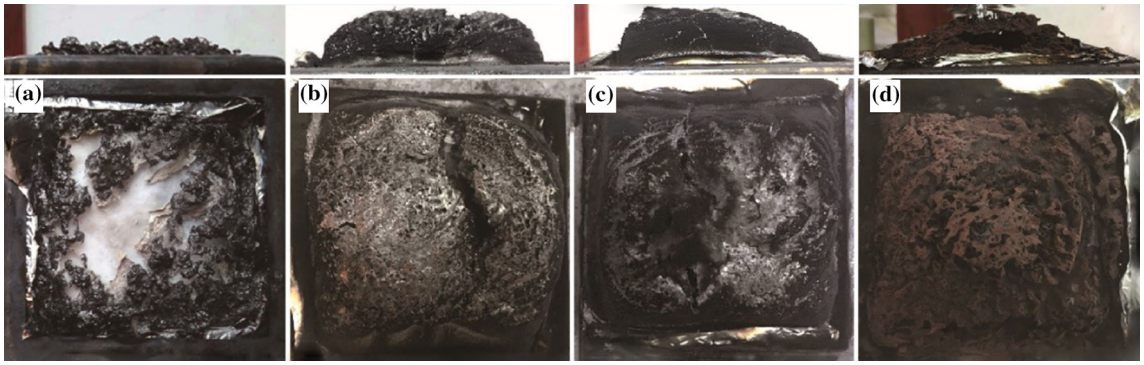

Fig. 4 Digital photographs of char residue of EP composites after CONE test: neat EP (**a**), 4APP/EP (**b**), 3APP/1AC-Fe_2O_3/EP (**c**) and 4AC-Fe_2O_3/EP (**d**)

AC-Fe_2O_3 and 3APP/1AC-Fe_2O_3 can all effectively lessen the production of smoke. Specially, the SPR value of 3APP/1AC-Fe_2O_3/EP is significantly lower than 4APP/EP during the first 150 s. This is because Fe in AC-Fe_2O_3 can catalyze the removal reaction of APP, which promotes the cross-linking of the pyrolysis product (polyphosphoric acid) with the epoxy resin and reduces the volatilization of small molecules and smoke. In addition, AC can act as a physical barrier, not only blocking the escape of small molecules inside the matrix, but also reducing the contact of the matrix with external flammable gases. After 150 s of irradiation, the char residue may be slowly oxidized and burned under high radiant power, so the TSP will increase. However, this will play a vital role in the fire rescue work and providing more chances for survival for trapped people.

In the mass loss curve (Fig. 3d), the amount of EP char residual increased after the addition of the flame retardant, while the sample 3# had the highest increase, which was higher than the pure EP by more than 150%. This is because the phosphoric acid produced by the decomposition of APP catalyzes the degradation of EP, and AC-Fe_2O_3 increases the carbon source to form a denser and regular char layer. This external char layer was so compact and dense that is effectively hindered the transmission of heat and internal flammable gases from the flame zone to the surface of the material, thereby reducing the possibility of continued combustion in the unburned area and improving the thermal insulation capability of EP samples.

From Fig. 4a, it can be seen that the pure EP samples have very little char residue, and they are aggregated into bolus, which also corresponds to severe dripping in vertical combustion. The char residual content of the flame-retarded EP sample significantly increased and became continuous, which also corresponded to the improvement of the dripping phenomenon in the vertical combustion.

The amount of char residue in the samples 2# and 6# (Fig. 4b, d) increased, but the inner char residue was loose and porous after breaking the surface. In comparison, the char residue of the sample 3# is smaller and denser, and there is no large collapse hole. This result shows that AC-Fe_2O_3 and APP can play a synergistic flame-retardant effect: promote the cross-linking of polymer molecules to form a better quality of char residue.

Figure 5 shows that the sample 3# has diffraction peaks for $Fe_4(P_2O_7)_3$ (PDF 36-0318) compared to the samples 1# and 6#. This demonstrates that Fe can react with the polyphosphoric acid formed by the decomposition of APP, and the generated pyrophosphate increases the content of condensed phase, thereby increasing the amount of char residual.

Dispersion of the APP and AC-Fe_2O_3 in EP matrix

The sample impact test was tested by SEM, as shown in Fig. 6. SEM and EDS mappings were used to further analyze the distribution of the flame retardant in the EP. It can be seen from Fig. 6b and c that there is a uniform distribution of particulate matter on the cross section. The EDS mapping shows that the elements contained in Fig. 6b

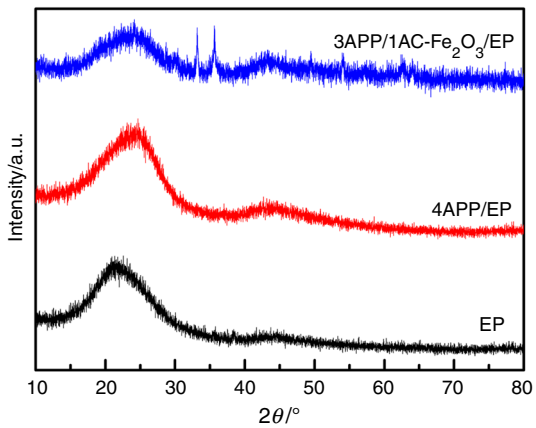

Fig. 5 XRD patterns of char residue of EP composites after CONE test

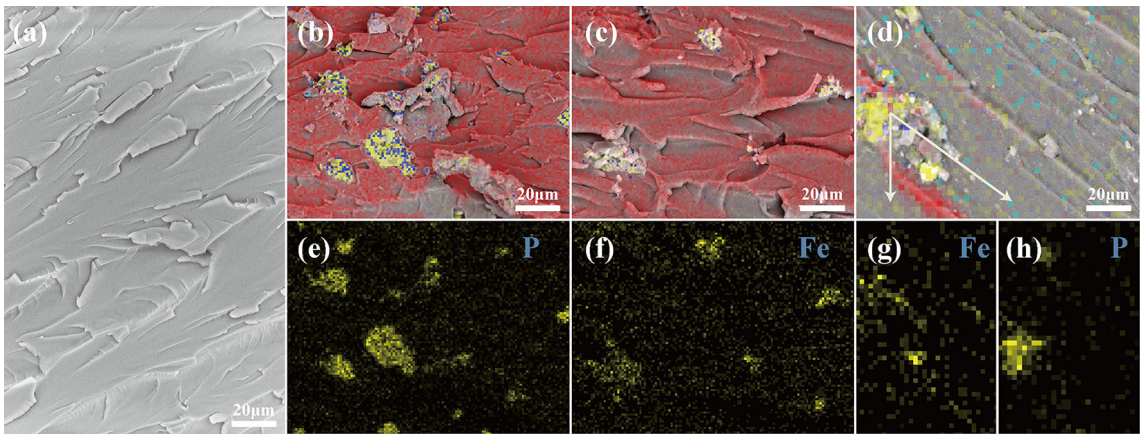

Fig. 6 SEM of EP (**a**), 4APP/EP (**b**), 4AC-Fe_2O_3/EP (**c**) and 3APP/1AC-Fe_2O_3/EP (**d**) and EDS mapping images of 4APP/EP (**e**), 4AC-Fe_2O_3/EP (**f**) and 3APP/1AC-Fe_2O_3/EP (**g**, **h**)

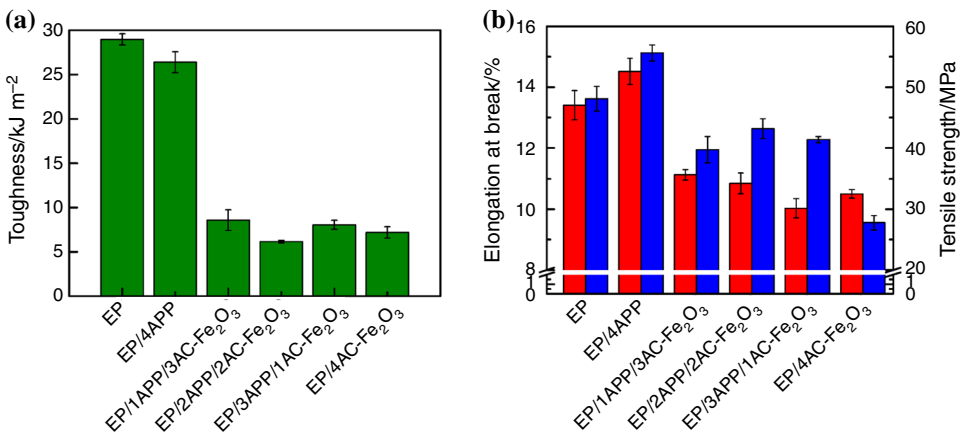

Fig. 7 Mechanical properties of EP composites: toughness (**a**), elongation at break and tensile strength (**b**)

and c correspond to the AC-Fe_2O_3 and APP, respectively. This proves that the particulate matter in Fig. 6b and c is AC-Fe_2O_3 and APP, respectively. Figure 6d shows SEM image of 3APP/1AC-Fe_2O_3/EP. It can be seen from the EDS mapping that the distribution of P and Fe corresponds to the SEM of 3APP/1AC-Fe_2O_3/EP, which proves that APP and AC-Fe_2O_3 are uniformly distributed in EP.

The data of toughness, elongation at break, and tensile strength of sample 1#–3# and 6# are shown in Fig. 7.

It can be seen from Fig. 7 that the mechanical properties of EP samples have decreased after the addition of the flame retardant. In particular, the sample 6# is about 60% lower than that of the samples 1# and 2#, but the elongation at break and the tensile strength are not significantly reduced. This may be due to the fact that the added flame retardant is an inorganic particle and has poor compatibility with the matrix.

It is worth noting that after the addition of four APP, the impact strength data of the sample 2# did not decline much, while the elongation at break and the tensile strength increased slightly. This may be due to the better compatibility between APP and EP, resulting in a homogeneous structure, making the EP sample structure more stable and less brittle.

Conclusions

In conclusion, flame-retardant EP composites were prepared using APP as an intumescent flame retardant and AC-Fe_2O_3 as a synergist. LOI and UL-94 test results showed that the simultaneous addition of APP and AC-Fe_2O_3 can improve the combustion performance of EP. The LOI of 3APP/1AC-Fe_2O_3/EP sample increased from 25.3 to 28.0% compared with the pure EP sample. The UL-94 test passed the V-0 rating without dripping, and the internal collapse of the char residual was significantly reduced. After analyzing the thermal decomposition behavior of above composites, it was found that thermal degradation rate of APP/AC-Fe_2O_3/EP decreases, with the advance of $T_{5\%}$, the decomposition rate decreased, and the there was an increase in char residual content. In addition,

cone calorimeter results indicated that Fe_2O_3 had synergistic effect with APP for suppressing the emission of smoke and toxic gases. It was deduced that the formation amount, intumescent degree, and compactness of the char were further improved because of the synergistic effect and catalytic action of AC-Fe_2O_3.

Acknowledgements The work was financially supported by the Key Basic Research Project of Hebei Province (No. 16961402D) and the Higher Education Science and Technology Research Project of Hebei Province (ZD2018011).

References

1. Yan L, Xu ZS, Wang XH, Deng N, Chu ZY. Preparation of a novel mono-component intumescent flame retardant for enhancing the flame retardancy and smoke suppression properties of epoxy resin. J Therm Anal Calorim. 2018;134(3):1505–19.
2. Feng Y, He C, Wen Y, Ye Y, Zhou X, Xie X, Mai YW. Synergy in flame-retarded epoxy resin. J Therm Anal Calorim. 2017;128(1):141–53.
3. Yu J, Li YT, Zhao CX, Xing YL, He D. Effect of different sizes of expandable graphite and synergic ammonium polyphosphate on the combustion performance of epoxy resin. Polym Mater Sci Eng. 2013;29(10):85–8.
4. Zhang MJ, Qu YH, Shen SG. Preparation of activated carbon spheres and its application in ammonium polyphosphate flame retardant epoxy resin. China Plast. 2017;31(9):127–32.
5. Wang F, Hao JW, Li ZS, Zou HF. Preparation of bamboo-based porous carbon materials and their synergistic flame-retardant effect for epoxy resin. Acta Polym Sin. 2015;8:897–905.
6. Zhang MJ, Wu WH, He SR, Wang X, Jiao YH, Qu HQ, Xu JZ. Synergistic flame retardant effects of activated carbon and molybdenum oxide in poly(vinyl chloride). Polym Int. 2018;67(4):445–52.
7. Gong J, Tian NN, Liu J, Yao K, Jiang ZW, Chen XC, Wen X, Mijowska E, Tang T. Synergistic effect of activated carbon and Ni_2O_3 in promoting the thermal stability and flame retardancy of polypropylene. Polym Degrad Stabil. 2014;99(5):18–26.
8. Wu N, Yang RJ. Effects of metal oxides on intumescent flame-retardant polypropylene. Polym Adv Technol. 2011;22(5):495–501.
9. Chen XL, Jiao CM, Wang Y. Synergistic effects of iron powder on intumescent flame retardant polypropylene system. Express Polym Lett. 2009;3(6):359–65.
10. Xu S, Wu WH, Cheng LY, Meng WH, Wang X, Qu HQ, Xu JZ. Preparation of cattail activated carbon suppored Fe_2O_3 and its flame retardant application in flexible polyvinyl chloride. Acta Mater Compos Sin. 2018;35(7):1745–53.
11. Liu Y, Wang JS, Deng CL, Wang DY, Song YP, Wang YZ. The synergistic flame-retardant effect of O-MMT on the intumescent flame-retardant PP/CA/APP systems. Polym Adv Technol. 2010;21(11):789–96.
12. Chen XL, Li M, Zhuo JL, Ma CY, Jiao CM. Influence of Fe_2O_3 on smoke suppression and thermal degradation properties in intumescent flame-retardant silicone rubber. J Therm Anal Calorim. 2015;123(1):439–48.
13. Gong J, Tian NN, Liu J, Yao K, Jiang ZW, Chen XC, Wen X, Mijowska E, Tang T. Synergistic effect of activated carbon and Ni_2O_3 in promoting the thermal stability and flame retardancy of polypropylene. Polym Degrad Stab. 2014;99(5):18–26.
14. Du BX, Fang ZP. Effects of carbon nanotubes on the thermal stability and flame retardancy of intumescent flame-retarded polypropylene. Polym Degrad Stabil. 2011;96(10):1725–31.
15. Zhao JS, Liu H, Zhang Q. Preparation of NiO nanoflakes under different calcination temperatures and their supercapacitive and optical properties. Appl Surf Sci. 2017;392:1097–106.
16. Deng LL, Shen MM, Yu J, Wu K, Ha CY. Preparation, characterization, and flame retardancy of novel rosin-based siloxane epoxy resins. Ind Eng Chem Res. 2012;51(24):8178–84.
17. Feng YZ, He CG, Wen YF, Ye YS, Zhou XP, Xie XL, Mai YW. Improving thermal and flame retardant properties of epoxy resin by functionalized graphene containing phosphorous, nitrogen and silicon elements. Compos Part A Appl S. 2017;103:74–83.
18. Yan W, Yu J, Zhang MQ, Wang T, Wen CZ, Qin SH, Huang WJ. Effect of multiwalled carbon nanotubes and phenethyl-bridged DOPO derivative on flame retardancy of epoxy resin. J Polym Res. 2018;25(3):72.
19. Liu LL, Huang YW, Yang Y, Ma JJ, Yang JX, Yin Q. Preparation of metal-phosphorus hybridized nanomaterials and the action of metal centers on the flame retardancy of epoxy resin. J Appl Polym Sci. 2017;2(11):45445–54.
20. Zhang L, Zhang KX, Wang X, Chen MJ, Xin F, Liu ZG. Surface morphology and electrochemical properties of brominated activated carbons. J Therm Anal Calorim. 2018;134(3):1637–46.
21. Puziy AM, Poddubnaya OI, Martínez-Alonso A, Castro-Muniz A, Suarez-Garcra F, Tascon JMD. Oxygen and phosphorus enriched carbons from lignocellulosic material. Carbon. 2007;45(10):1941–50.
22. Ridder DJD, Verliefde ARD, Schoutteten K, van der Linden B, Heijman SGJ, Beurroies I, Denoyel R, Amy GL, van Dijk JC. Relation between interfacial energy and adsorption of organic micropollutants onto activated carbon. Carbon. 2013;53(1):153–60.